Food Chemistry 171 (2015) 292–297

Contents lists available at ScienceDirect

Food Chemistry

journal homepage: www.elsevier.com/locate/foodchem

Analytical Methods

Synthesis and characterization of core–shell magnetic molecularly imprinted polymers for solid-phase extraction and determination of Rhodamine B in food

Xiaomeng Su [a], Xiaoyan Li [a,*], Junjie Li [b], Min Liu [a], Fuhou Lei [a], Xuecai Tan [a], Pengfei Li [a], Weiqiang Luo [a]

[a] School of Chemistry and Chemical Engineering, Guangxi University for Nationalities, Key Laboratory of Chemistry and Engineering of Forest Products, Nanning, Guangxi 530008, China
[b] School of Chemistry and Chemical Engineering, Guangxi University, Nanning, Guangxi 530004, China

ARTICLE INFO

Article history:
Received 20 February 2014
Received in revised form 4 September 2014
Accepted 6 September 2014
Available online 16 September 2014

Keywords:
Core–shell magnetic nanoparticles
Molecularly imprinted polymers
Solid-phase extraction
Rhodamine B
Food

ABSTRACT

Core–shell magnetic molecularly imprinted polymers (MIPs) nanoparticles (NPs), in which a Rhodamine B-imprinted layer was coated on Fe_3O_4 NPs. were synthesized. First, Fe_3O_4 NPs were prepared by a coprecipitation method. Then, amino-modified Fe_3O_4 NPs (Fe_3O_4@SiO_2-NH_2) was prepared. Finally, the MIPs were coated on the Fe_3O_4@SiO_2-NH_2 surface by the copolymerization with functional monomer, acrylamide, using a cross-linking agent, ethylene glycol dimethacrylate; an initiator, azobisisobutyronitrile and a template molecule, Rhodamine B. The Fe_3O_4@MIPs were characterized using a scanning electron microscope, Fourier transform infrared spectrometer, vibrating sample magnetometer, and re-binding experiments. The Fe_3O_4@MIPs showed a fast adsorption equilibrium, a highly improved imprinting capacity, and significant selectivity; they could be used as a solid-phase extraction material and detect illegal addition Rhodamine B in food. A method was developed for the selective isolation and enrichment of Rhodamine B in food samples with recoveries in the range 78.47–101.6% and the relative standard deviation was <2%.

1. Introduction

Rhodamine B, a synthetic dye, has been used for fluorescent labelling (Longmire et al., 2008; Nguyen & Francis, 2003) and food colouring, because of his intense pink colour. However, Rhodamine B has been found to cause cancer in rats and mice through multiple tests (International Agency for Research on Cancer, http://www.iarc.fr/). Now Rhodamine B is forbidden to use as a food colouring. China Food and Drug Administration published an emergency notification to forbid it in food as well (China Food and Drug Administration, http://www.sfda.gov.cn/WS01/CL0001/).

Because of the complexity of food matrices and low concentration of Rhodamine B in food, the analysis of Rhodamine B requires extensive sample pretreatment, for example, liquid liquid extraction and solid-phase extraction (SPE) (Soylak, Unsal, Yilmaz, & Tuzen, 2011; Yan, Liu, Du, Yang, & Row, 2010). However, these methods lack selective adsorption ability. Molecularly imprinted polymer (MIP) adsorbents are more selective than traditional SPE adsorbents; therefore, MIPs have attracted much attention in the past decade as an attractive alternative for the analysis of complex samples (Baggiani et al., 2009; Takeuchi, Fukuma, & Matsui, 1999).

MIPs exhibit high affinity and selectivity for a given target. MIPs are obtained by the polymerization of functional monomers using a cross-linker around a template. The removal of template leaves behind recognition sites of functional and shape complementary to the template (Sun, He, Zhang, & Chen, 2009; Yamazaki, Ohta, Yanai, & Sode, 2003). Compared to antibodies, enzymes, or biological molecules, MIPs show inherent advantages: First, the preparation of MIPs is quite simple and economical. Second, MIPs provided good physical and chemical stability. Finally, MIPs can be used in harsh chemical environments without loss of blinding properties. Most of the MIPs have been synthesized by bulk and precipitation polymerization methods (Li, Wang, Zhang, Qi, & Deng, 2008; Wang, Wang, Gong, & Chang, 2003), followed by a grinding and sieving to obtain the desired particles; however, they have drawbacks in some applications, for example, heterogeneous distribution of the binding sites, and poor site accessibility to the target molecules, because the template and functionality are totally embedded in the polymer matrices. These drawbacks lead to unfavorable kinetics of the sorption/desorption process and slow mass transfer. To solve these problems, surface-imprinted core–shell nanoparticles (NPs) have been studied (Deng, Qi, Deng, Zhang, &

* Corresponding author. Tel.: +86 7713260558.
E-mail address: lixiaoyan73515@163.com (X. Li).

http://dx.doi.org/10.1016/j.foodchem.2014.09.024
0308-8146/

Zhao, 2008; Liu, Lei, Zhai, & Li, 2012; Neoh & Kang, 2012; Tan & Tong, 2007; Zhang et al., 2010).

Magnetic field-based separations using magnetic nano and microparticles have received great attention for their superior characteristics such as good dispersion, fast and effective binding of targets, and reversible and controllable flocculation (Chatterjee, Haik, & Chen, 2003; Kan et al., 2010; Li et al., 2012). The magnetic separation process can be performed directly in crude samples containing suspended solid or other biological particles in a rapid and easy manner, thus greatly facilitating the lab work (Chen, Deng, & Zhang, 2010; Xu et al., 2012; Zhang, Tan, Hu, & Li, 2011). Moreover, the power and efficiency of magnetic separation procedures can be used in large-scale operations. Surface modification of magnetic NPs is essential for many applications (Bagheri, Daliri, & Roostaie, 2013; Gai, Qu, Zhang, & Zhang, 2011; Gao et al., 2011; Li, He, Chen, & Zhang, 2009). Magnetic NPs coated with MIPs can be used to separate and concentrate chemicals conveniently using an external magnetic field. Therefore, a combination of magnetic separation and molecular imprinting would provide a powerful analytical tool with simplicity, flexibility, and selectivity.

In this study, we prepared magnetic Fe_3O_4@MIPs with uniform core–shell structure by combining surface imprinting and nanotechniques. First, Fe_3O_4 NPs were prepared by a coprecipitation method. Then Fe_3O_4@SiO_2-NH_2 was prepared by coupling the aminosilica groups on the Fe_3O_4 surface through (3-aminopropyl)triethoxysilane (APTES).The MIPs were coated on the Fe_3O_4@SiO_2-NH_2 surface by the copolymerization of the amino end groups with functional monomer, acrylamide (AM), using a cross-linking agent, ethylene glycol dimethacrylate (EGDMA); an initiator, azobisisobutyronitrile (AIBN); and a template molecule, Rhodamine B. The Fe_3O_4@MIPs were characterized using a scanning electron microscope (SEM), Fourier transform infrared (FT-IR) spectrometer, and vibrating sample magnetometer (VSM). The adsorptive capacity was determined by adsorption equilibrium experiment and Scatchard analysis. The selectivity of Fe_3O_4@MIPs NPs was studied by the different rebinding capability of Rhodamine B and the related different representatives of Rhodamine B. The Fe_3O_4@MIPs were able to adsorb Rhodamine B specifically and could be applied to separate and enrich Rhodamine B in food.

2. Experimental

2.1. Chemicals

APTES was obtained from Kayon Biological Technology Co. Ltd. (Shanghai, China). AM was obtained from Hefei Biosharp Co. Ltd. (Anhui, China). EGDMA was obtained from Fushun Anxin Chemical Co. Ltd. (Liaoning, China). Rhodamine B and Rhodamine 6G were obtained from Chemical Reagent Co. Ltd. (Shanghai, China). AIBN was obtained from No. 4 Reagent & H.V. Chemical Co. Ltd. (Shanghai, China). Methanol, ethanol, n-hexane, acetone, and glacial acetic acid were obtained from Guanghua Science and Technology Co. Ltd. (Guangdong, China). Acetonitrile was obtained from Fisher Scientific (USA). Iron(II) dichloride and iron(III) chloride were obtained from Chemicals Co. Ltd. (Tianjin, China). Highly purified water was obtained from a Pro Water System (Millipore Co. Ltd., USA). All the reagents used were of analytical or high performance liquid chromatography (HPLC) grade and used as received without further purification. The food samples were randomly obtained from some local supermarkets (Nanning, China).

2.2. Instrumentation and conditions

The morphologies of Fe_3O_4, Fe_3O_4@SiO_2-NH_2, and Fe_3O_4@MIPs were observed using a Hitachi Su8020 SEM. The infrared spectra were recorded using a Magna IR550 (II) FT-IR spectrometer. The UV–visible absorption spectra were recorded using a UV1800 UV–visible spectrophotometer (Shimadzu, Japan). The magnetic properties were evaluated using a 7410 VSM (Lake Shore Company, USA).The HPLC analyses were performed using an Agilent 1260 HPLC including a G1314B variable wavelength UV–visible detector, a G1316A column oven, and a G1311C quaternary pump. A Phenomenex Gemini-C18 (5 μm particle size, 250 × 4.6 mm) analytical column was used for the separation of analytes. The mobile phase was acetonitrile/H_2O (8/2, v/v), and the flow rate was 1.0 mL/min at 35 °C. The injection volume was 20 μL, and the wavelength of the detector was monitored at 556 nm.

2.3. Preparation of amino-modified magnetic NPs

2.3.1. Synthesis of Fe_3O_4 NPs

$FeCl_2{\cdot}4H_2O$ (2.0 g) and $FeCl_3{\cdot}6H_2O$ (5.3 g) were added to 150 mL of highly purified water in a three-neck flask under nitrogen atmosphere. The mixture was stirred by the Teflon paddle and heated by the heating jacket. When the temperature reached 80 °C under stirring, 25 mL ammonium solution was added dropwise into the flask and stirred for 6 h. The product was separated from the reaction mixture using a Nd-Fe-B permanent magnet. The product was added to a 100 mL 0.2 M aqueous solution of sodium citrate under ultrasonic vibration for 5 min. Then, the product was separated by a magnet. The black precipitate was washed with highly purified water until the pH of the solution was 7, washed with ethanol, and dried under vacuum at 60 °C.

2.3.2. Synthesis of amino-modified Fe_3O_4 NPs (Fe_3O_4@SiO_2-NH_2)

The Fe_3O_4 NPs (0.4 g) were dispersed in 150 mL ethanol/H_2O (1:1, v/v). Then resulting mixture was stirred vigorously (300 rpm), and 0.5 mL APTES was added dropwise. The pH was adjusted to 4.0 with glacial acetic acid. Then, the reaction mixture was purged with nitrogen and stirred at 60 °C for 3 h. The product was separated using a magnet. The black precipitate was washed with highly purified water until the pH of the solution was 7 and dried under vacuum to afford amino-modified Fe_3O_4 NPs.

2.3.3. Preparation of the core–shell Fe_3O_4@MIPs and Fe_3O_4@NIPs

0.1 g Fe_3O_4@SiO_2-NH_2, 0.2395 g (0.5 mmol) Rhodamine B, and 0.1422 g AM (2 mmol) were added to 30 mL acetonitrile under ultrasonic vibration for 15 min, and then the mixture was placed in dark for 12 h to form a template-monomer complex. EGDMA (1.981 g) (10 mmol) and AIBN (0.06 g) were homogeneously dispersed by ultrasonic vibration for 15 min, and then the solution was transferred to a 250 mL three-necked flask. Then, 70 mL acetonitrile was added. The reaction mixture was purged with nitrogen and stirred at 60 °C for 8 h, followed by at 75–78 °C for 2 h. Then, Rhodamine B Fe_3O_4@MIPs were obtained. The Fe_3O_4@MIPs were washed with copious amount of acetonitrile, and the Rhodamine B templates in the product were removed by methanol/AcOH (9:1, v/v) by Soxhlet extraction. Finally, the product was washed with methanol until neutral and dried in vacuum.

Non-imprinted Fe_3O_4@NIPs were prepared by the same method except for the template Rhodamine B.

2.4. Study of physical characterization and extraction capability

2.4.1. Rebinding experiments of Fe_3O_4@MIPs and Fe_3O_4@NIPs

In the adsorption kinetics experiment, 25.0 mg Fe_3O_4@MIPs or Fe_3O_4@NIPs was added to a 10.0 mL, 1 mM acetonitrile solution of Rhodamine B and incubated (shaken at 80 rpm by the water bath incubator shaker) at regular time intervals from 5 min to 120 min at room temperature. After the supernatant and polymers were separated using an external magnetic field, the concentration of Rhodamine B in the supernatant and the amount of Rhodamine

B bound to the Fe_3O_4@MIPs or Fe_3O_4@NIPs were measured by a UV–visible spectrophotometer at 556 nm.

In the isothermal binding experiment, 25.0 mg Fe_3O_4@MIPs or Fe_3O_4@NIPs were added to a 10.0 mL acetonitrile solution of Rhodamine B in the concentration range 0.05–0.7 mg/mL and incubated for 30 min at room temperature. The supernatant and polymers were separated using an external magnetic field, and the concentration of Rhodamine B in the supernatant was analysed by UV–visible spectroscopy at 556 nm.

2.4.2. Specific recognition of Fe_3O_4@MIPs and Fe_3O_4@NIPs

Fe_3O_4@MIPs or Fe_3O_4@NIPs (25.0 mg) were added to a 10.0 mL, 1 mM acetonitrile solution of Rhodamine B or Rhodamine 6G for each compound. After incubating for 30 min at room temperature, the supernatant and polymers were separated using an external magnetic field, and the amount of Rhodamine B and its analog in the supernatant was analysed by UV–visible spectroscopy.

2.4.3. Determination of Rhodamine B in samples

All the selected food samples were free of Rhodamine B, and the spiking concentrations were 5, 10, and 20 mg/kg.

The food sample (1.0 g) was accurately weighed in a 25 mL conical flask with a stopper, and then a 10.0 mL standard solution of Rhodamine B was added. After ultrasonic treatment for 5–10 min, 3.0 mL of the supernatant solution was added to another 25 mL conical flask. Typically, 15.0 mg of Fe_3O_4@MIPs were added and shaken at 80 rpm for 30 min at room temperature. The supernatant and polymers were separated using an external magnetic field. After discarding the supernatant solution, the Fe_3O_4@MIPs were washed with 1th mL of n-hexane/acetone (8:2, v/v) to reduce or eliminate the co-extracted impurities. Then, the Rhodamine B was eluted from the Fe_3O_4@MIPs with 3×2.0 mL of methanol, and the combined elute was evaporated to dryness under a stream of nitrogen. The residue was added to 2.0 mL acetonitrile/water (8:2, v/v), and filtered through a 0.45 μm organic membrane and measured by HPLC.

3. Results and discussion

3.1. Preparation of imprinted magnetic nanoparticles

The multistep synthesis procedure of Fe_3O_4@MIPs NPs is illustrated in Fig. 1. Fe_3O_4@NPs were synthesized by a co-precipitation method. The surface of the Fe_3O_4 NPs was then modified using APTES to afford Fe_3O_4@SiO_2-NH_2. This decreased the magnetic dipole attraction between the magnetite NPs, thus increasing the dispersion of magnetite NPs; moreover, the silica-NH_2 surface can be easily modified with different groups for bioconjugation purpose (Wang, Wang, He, Zhang, & Chen, 2009; Yi, Lee, & Ying, 2006). Further, the surface amino groups of Fe_3O_4@SiO_2-NH_2 were reacted with the functional monomer (AM).

In addition, the Fe_3O_4 NPs had a small diameter with an extremely high surface-to-volume ratio, and most of the templates were easily placed on the surface of the Fe_3O_4 NPs. The MIPs were coated on the surface of Fe_3O_4@SiO_2-NH_2 by the copolymerization of functional monomer (AM) using a cross-linking agent (EGDMA), an initiator (AIBN) and a template molecule (Rhodamine B). Finally, after the templates were removed to afford the Fe_3O_4@MIPs NPs. Therefore, Fe_3O_4@MIPs NPs may provide access to the recognition sites to the template molecule and can be easily separated using an external magnetic field. For comparison purposes, the Fe_3O_4@NIPs NPs were also prepared using an identical procedure, but without the adding the template Rhodamine B.

3.2. Characterization of imprinted magnetic nanoparticles

The products of Fe_3O_4, Fe_3O_4@SiO_2-NH_2, Fe_3O_4@MIPs, and Fe_3O_4@NIPs were investigated by FT-IR spectroscopy (Fig. 2). The characteristic absorption bands at 585 and 631 cm^{-1} are attributed to the Fe–O stretching vibration (Fig. 2A). After the modification of aminosilica with APTES on the pure Fe_3O_4 surface, the Si–O–Si stretching vibration was observed at ~1060 cm^{-1}, and the N–H and O–H bending vibrations were observed at ~1629 cm^{-1} (Fig. 2B). Moreover, because of the N–H stretching vibration, the peak area increased at ~3500–3300 cm^{-1}. Fig. 2C and D shows the peaks of C=O stretching vibration at ~1731 cm^{-1} and C–H stretching vibration of the methyl group at ~2924 cm^{-1}, indicating that the AM-EGDMA layer was successfully formed on the surface of Fe_3O_4@SiO_2-NH_2. In addition, Fe_3O_4@MIPs and Fe_3O_4@NIPs showed almost the same characteristic absorption bands, indicating the complete removal of templates. These results indicate the successful preparation of MIPs and NIPs.

The sizes of Fe_3O_4 and Fe_3O_4@SiO_2-NH_2 were examined using a SEM. The average diameter of Fe_3O_4 was 20 nm. After modifying Fe_3O_4 with APTES, the diameter of the Fe_3O_4@SiO_2-NH_2 increased to ~50 nm, indicating that the coupling of APTES on the Fe_3O_4 surface successfully afforded a core–shell structure. The surface of the Fe_3O_4@MIPs is uneven with many holes; thus facilitating the adsorption of template molecules. In contrast, the surface of Fe_3O_4@NIPs is smooth, thus lacking effective adsorption sites.

The magnetic properties of the MIPs were studied by VSM: the magnetic hysteresis loops of the Fe_3O_4, Fe_3O_4@SiO_2-NH_2, and Fe_3O_4@MIPs at room temperature. No hysteresis phenomenon was observed, and the remanence and coercivity are zero, indicating that the samples are superparamagnetic. The saturation magnetization values of Fe_3O_4, Fe_3O_4@SiO_2-NH_2, and Fe_3O_4@MIPs were 24.8, 22.0, and 21.2 emu/g, respectively. The magnetization values decreased with increasing core–shell structure. Although the saturation magnetization of Fe_3O_4@MIPs reduced by 3.6 emu/g compared to the pure Fe_3O_4, the Fe_3O_4@MIPs still showed strong magnetism and separated rapidly using an external magnetic field.

3.3. Binding properties of imprinted magnetic NPs

3.3.1. Adsorption of Fe_3O_4@MIPs and Fe_3O_4@NIPs NPS

To find a suitable solvent for the rebinding of templates, several types of solvents were investigated. The results showed that the addition of water or methanol disturbed the specific binding effect of the Fe_3O_4@MIPs, probably because the strong polarity of water or methanol destroyed the hydrogen bond between the Fe_3O_4@MIPs and template molecules. In addition, acetonitrile, showed the best result and therefore was used in further studies.

The recognition ability of Fe_3O_4@MIPs NPs towards Rhodamine B was investigated by adsorption kinetics, adsorption thermodynamics, and Scatchard analyses. The adsorption kinetics of 1 mmol/L Rhodamine B solution on Fe_3O_4@MIPs and Fe_3O_4@NIPs are shown in Fig. 3(A). The adsorption capacity increased with time, and the Fe_3O_4@MIPs showed a fast adsorption rate.

The adsorption capacity increased rapidly in the first 15 min and almost reached equilibrium after 30 min. The equilibrium time in this study is also shorter than the other imprinting technology for Rhodamine B, because most of the recognition sites of the imprinted polymers are on the surface of the imprinted magnetic NPs. The Fe_3O_4@MIPs showed high adsorption efficiency and overcome some shortcomings of traditional molecularly imprinted materials.

The binding isotherms of Rhodamine B onto Fe_3O_4@MIPs and Fe_3O_4@NIPs were determined in the concentration range 0.1–0.7 mg/mL (initial concentration), and the results are shown in Fig. 3(B). The amount of Rhodamine B bound to the Fe_3O_4@MIPs

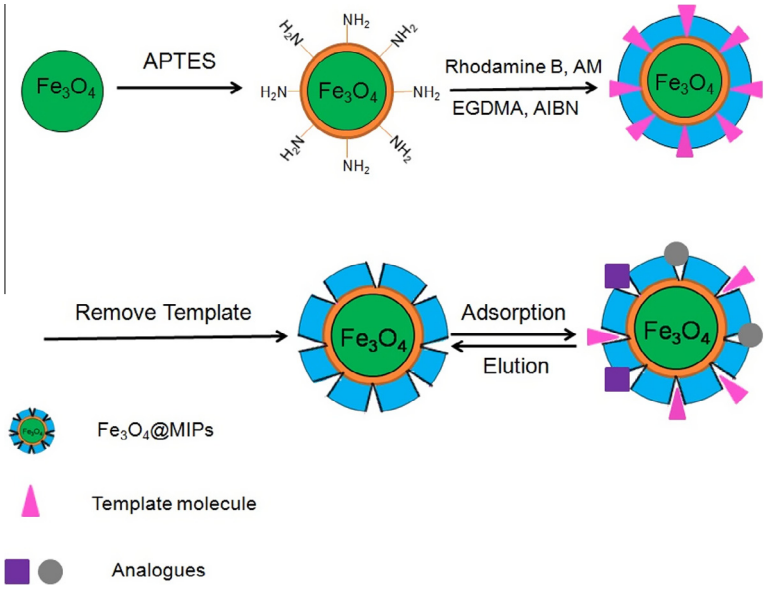

Fig. 1. Schematic procedure of the preparation of Fe_3O_4@MIPs NPs.

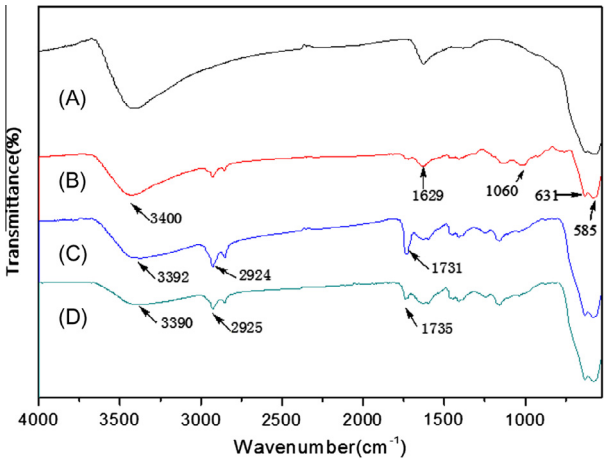

Fig. 2. FT-IR spectra of Fe_3O_4 (A), Fe_3O_4@SiO_2-NH_2 (B), Fe_3O_4@MIPs (C) and Fe_3O_4@NIPs (D).

increased rapidly with increasing initial concentration <0.5 mg/mL. However, when the initial concentration was >0.4 mg/mL, the adsorption curve became relatively flat and reached its saturation at a high Rhodamine B concentration. The amount of Rhodamine B bound to the Fe_3O_4@MIPs was significantly higher than that of the Fe_3O_4@NIPs at the same initial concentration.

To further analyse the experimental data, the Scatchard equation was used to estimate the binding properties of the Fe_3O_4@MIPs. The Scatchard equation is expressed as follows:

$$Q/C_e = (Q_{max} - Q)/K_d$$

where Q is the amount of Rhodamine B bound to Fe_3O_4@MIPs at equilibrium, Q_{max} is the apparent maximum adsorption capacity, C_e is the free Rhodamine B concentration at equilibrium, and K_d is the dissociation constant. The values of K_d and Q_{max} can be calculated from the slope and intercept of the linear line plotted in Q/C_e vs. Q. The Scatchard analysis for the Fe_3O_4@MIPs was performed as shown in Fig. 3(C).

The Scatchard plot for Fe_3O_4@MIPs was not a single linear curve, but consisted of two linear parts with different slopes. The linear regression equation for the left part of the curve was $Q/C_e = -130.62\ Q + 7765.1$ ($r = 0.9997$). The K_d and Q_{max} were calculated to be 0.0077 mg/mL and 59.44 mg/g at high affinity binding sites, respectively. The linear regression equation for the right part of this curve was $Q/C_e = -8.6878\ Q + 909.05$ ($r = 0.9744$). The K_d and Q_{max} were calculated to be 0.1151 mg/mL and 104.6 mg/g at low affinity binding sites, respectively.

3.3.2. Molecular recognition of Fe_3O_4@MIPs and Fe_3O_4@NIPs NPS

To confirm that the Fe_3O_4@MIPs are selective for Rhodamine B, Rhodamine 6G was used as the structural analog. The adsorption of the Fe_3O_4@MIPs and Fe_3O_4@NIPs for the solutions of Rhodamine B and Rhodamine 6G in 10 mL, 1 mM acetonitrile are shown in Fig. 4.

The specificity of Fe_3O_4@MIPs can be estimated by the imprinting factor of the selected Rhodamine B between Fe_3O_4@MIPs and Fe_3O_4@NIPs. The imprinting factor α was determined according to the following formula:

$$\alpha = Q_{Fe_3O_4@MIPs}/Q_{Fe_3O_4@NIPs}$$

where $Q_{Fe_3O_4@MIPs}$ and $Q_{Fe_3O_4@NIPs}$ are the adsorption capacity of the same analyte, Fe_3O_4@MIPs and Fe_3O_4@NIPs, respectively.

As shown in Fig. 4, the Fe_3O_4@MIPs revealed a significantly higher adsorption amount of Rhodamine B than its analog; however, the Fe_3O_4@NIPs did not show such a difference, indicating that the template molecule had a relatively higher affinity for the imprinted polymer than its analog. Moreover, the α of Rhodamine B was also much higher than its analog, indicating that the Fe_3O_4@MIPs well recognized Rhodamine B. Although Rhodamine B and Rhodamine 6G have similar scaffold (xanthene), the differences in their spatial structures and functional groups caused a mismatch in the holes and binding sites leading to less adsorption of Rhodamine 6G and an imprinting factor(α) < 1. These results indicate the excellent imprinting efficiency of the present method.

3.3.3. Selective enrichment and purification of Rhodamine B in food samples

The prepared Fe_3O_4@MIPs were applied for the selective isolation and enrichment of Rhodamine B in food samples. For example, in the pepper sample, the spiked concentration for Rhodamine B was 10 mg/kg, and the methanol elution of the adsorbed Rhodamine B on the Fe_3O_4@MIPs after the adsorption of the pepper sample is shown in Fig. 5.

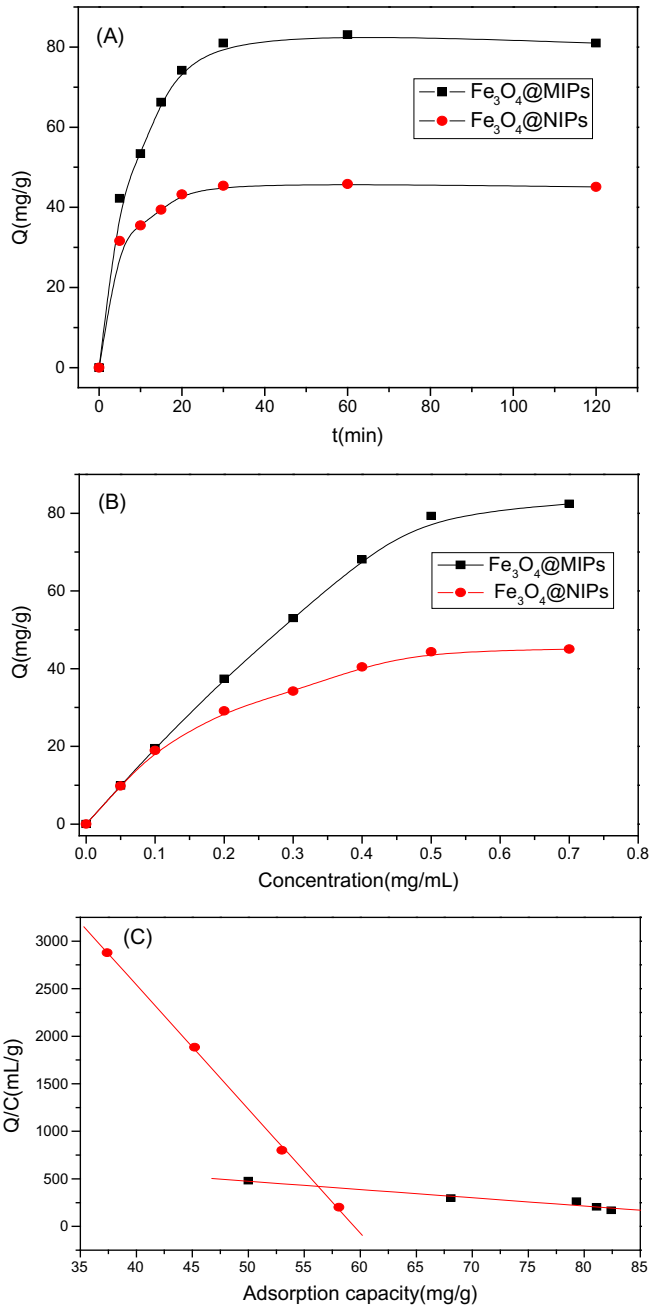

Fig. 3. Adsorption kinetics of Fe_3O_4@MIPs and Fe_3O_4@NIPs (A); adsorption isotherm of Rhodamine B onto Fe_3O_4@MIPs and Fe_3O_4@NIPs (B); Scatchard plot to estimate the binding mechanism of Fe_3O_4@MIPs towards Rhodamine B (C).

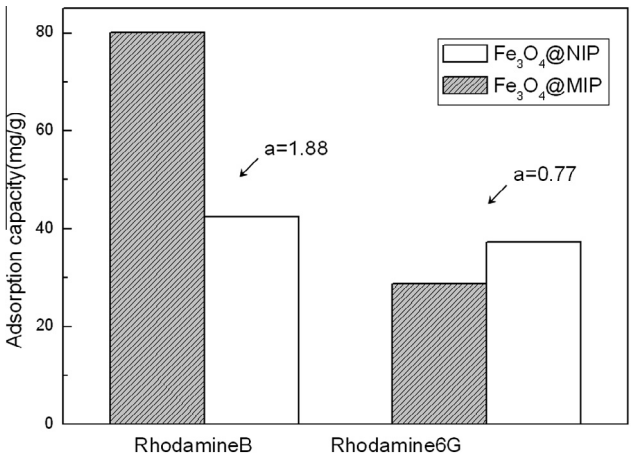

Fig. 4. The competitive adsorption capacity of Rhodamine B and Rhodamine 6G onto Fe_3O_4@MIPs and Fe_3O_4@NIPs.

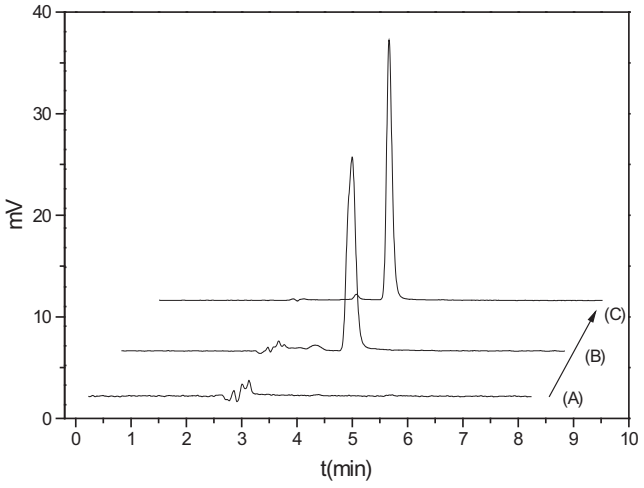

Fig. 5. Chromatograms of pepper sample (A), spiked sample of Rhodamine B (B), and elution fraction (C).

Table 1
Recovery and precision of Rhodamine B in the different spiked food samples ($n = 5$).

Samples	The level of spiked with Rhodamine B (mg/kg)	Recovery (%)	RSD (%)
Dyed pink melon seeds	5	78.47	1.71
Pepper	10	100.3	1.59
Candied purple potato	20	101.6	0.19

Fig. 5(A) shows the chromatogram of the pepper sample without Rhodamine B, the interference of substrate was distributed between 2.81 min and 3.22 min. Fig. 5(B) shows the chromatogram of the pepper sample spiked with standard Rhodamine B which appeared at 4.13 min. Fig. 5(C) shows the chromatogram of elution fraction. After the enrichment of the spiked pepper sample with the Fe_3O_4@MIPs and elution with methanol, the peak for Rhodamine B also appeared distinctly at 4.13 min, and other irrelevant compounds in the sample were almost eliminated. The results indicate that Rhodamine B was selectively enriched and purified in the pepper sample.

To evaluate the application of the developed method, dyed pink melon seed, pepper and candied purple potato were used for the spiked recovery experiments. As shown in Table 1, all selected samples were free of Rhodamine B. In the food samples, the recovery rates of Rhodamine B were 78.47–101.6% with a relative standard deviation less than 2%. The results indicate that the developed Fe_3O_4@MIPs–SPE method can selectively enrich Rhodamine B in the complex samples.

The concentration range of the calibration curve was 0.1–8.0 μg/mL with a highly linear regression coefficient (R^2 = 0.9998). The method detection limit of Rhodamine B was 3.4 μg/L (the signal-to-noise ratio was three). These results indicate that the Fe_3O_4@MIPs can be used for the selective adsorption separation and determination of Rhodamine B in food samples.

4. Conclusion

In this study, MIPs were synthesized with a MIP layer on Fe_3O_4@SiO_2-NH_2 NPs with a uniform core–shell structure by surface imprinting and nanotechniques. The Fe_3O_4@MIPs just needed ~30 min to reach the adsorption equilibrium with an improved imprinting capacity and a maximum adsorption amount of 104.6 mg/g. The Fe_3O_4@MIPs showed significant selectivity ($\alpha = 1.88$). The successful selective separation and enrichment of Rhodamine B in food samples indicate that the Fe_3O_4@MIPs may be used as a solid-phase extraction material and applied to detect the illegal addition of Rhodamine B in food.

Acknowledgement

This work was supported by the National Natural Science Foundation of China (Nos. 21165003, 31360162 and 21365004).

References

Baggiani, C., Anfossi, L., Baravalle, P., Giovannoli, C., Giraudi, G., Barolo, C., et al. (2009). Determination of banned Sudan dyes in food samples by molecularly imprinted solid phase extraction-high performance liquid chromatography. *Journal of Separation Science, 32*, 3292–3300.

Bagheri, H., Daliri, R., & Roostaie, A. (2013). A novel magnetic poly(aniline-naphthylamine)-based nanocomposite for micro solid phase extraction of rhodamine B. *Analytica Chimica Acta, 794*, 38–46.

Chatterjee, J., Haik, Y., & Chen, C. J. (2003). Biodegradable magnetic gel: Synthesis and characterization. *Colloid and Polymer Science, 281*, 892–896.

Chen, H. M., Deng, C. H., & Zhang, X. M. (2010). Synthesis of Fe_3O_4@SiO_2@PMMA core–shell–shell magnetic microspheres for highly efficient enrichment of peptides and proteins for MALDI-ToF MS analysis. *Angewandte Chemie International Edition, 49*, 607–611.

China Food and Drug Administration (CFDA). Available from http://www.sfda.gov.cn/WS01/CL0001/.

Deng, Y. H., Qi, D. W., Deng, C. H., Zhang, X. M., & Zhao, D. Y. (2008). Superparamagnetic high-magnetization microspheres with an Fe_3O_4@SiO_2 core and perpendicularly aligned mesoporous SiO_2 shell for removal of microcystins. *Journal of American Chemistry Society, 130*(1), 28–29.

Gai, Q. Q., Qu, F., Zhang, T., & Zhang, Y. K. (2011). Integration of carboxyl modified magnetic particles and aqueous two-phase extraction for selective separation of proteins. *Talanta, 85*, 304–309.

Gao, R. X., Kong, X., Wang, X., He, X. W., Chen, L. X., & Zhang, Y. K. (2011). Preparation and characterization of uniformly sized molecularly imprinted polymers functionalized with core–shell magnetic nanoparticles for the recognition and enrichment of protein. *Journal of Materials Chemistry, 21*, 17863–17871.

International Agency for Research on Cancer (IARC). Available from http://www.iarc.fr/.

Kan, X. W., Zhao, Q., Shao, D. L., Geng, Z. R., Wang, Z. L., & Zhu, J. J. (2010). Preparation and recognition properties of bovine hemoglobin magnetic molecularly imprinted polymers. *The Journal of Physical Chemistry B, 114*(11), 3999–4004.

Li, Y. H., Wang, Y. Q., Zhang, S. Y., Qi, X. L., & Deng, A. P. (2008). Development of a group selective molecularly imprinted polymers based solid phase extraction of malachite green. *Chemical Research and Application in Chinese, 20*(9), 1163–1165.

Li, L., He, X. W., Chen, L. X., & Zhang, Y. K. (2009). Preparation of core–shell magnetic molecularly imprinted polymer nanoparticles for recognition of bovine hemoglobin. *Chemistry – An Asian Journal, 4*, 286–293.

Li, X. X., Pan, J. M., Dai, J. D., Dai, X. H., Xu, L. C., Wei, X., et al. (2012). Surface molecular imprinting onto magnetic yeast composites via atom transfer radical polymerization for selective recognition of cefalexin. *Chemical Engineering Journal, 198–199*, 503–511.

Liu, H. Q., Lei, X. L., Zhai, Y. Y., & Li, L. (2012). Electrospun nanofiber membranes containing molecularly imprinted polymer (MIP) for Rhodamine B (RhB). *Advances in Chemical Engineering and Science, 2*, 266–274.

Longmire, M. R., Ogawa, M., Hama, Y., Kosaka, N., Regino, C. A. S., Choyke, P. L., et al. (2008). Determination of optimal rhodamine fluorophore for in vivo optical imaging. *Bioconjugate Chemistry, 19*(8), 1735–1742.

Neoh, K. G., & Kang, E. T. (2012). Surface modification of magnetic nanoparticles for stem cell labeling. *Soft Matter, 8*, 2057–2069.

Nguyen, T., & Francis, M. B. (2003). Practical synthetic route to functionalized rhodamine dyes. *Organic Letters, 5*(18), 3245–3248.

Sun, X. L., He, X. W., Zhang, Y. K., & Chen, L. X. (2009). Determination of tetracyclines in food samples by molecularly imprinted monolithic column coupling with high performance liquid chromatography. *Talanta, 79*, 926–934.

Soylak, M., Unsal, Y. E., Yilmaz, E., & Tuzen, M. (2011). Determination of Rhodamine B in soft drink, waste water and lipstick samples after solid phase extraction. *Food and Chemical Toxicology, 49*, 1796–1799.

Takeuchi, T., Fukuma, D., & Matsui, J. (1999). Combinatorial molecular imprinting: An approach to synthetic polymer receptors. *Analytical Chemistry, 71*(2), 285–290.

Tan, C., & Tong, Y. (2007). Preparation of superparamagnetic ribonuclease a surface-imprinted submicrometer particles for protein recognition in aqueous media. *Analytical Chemistry, 79*(1), 299–306.

Wang, S., Wang, Y. Z., Gong, G. Q., & Chang, X. J. (2003). Studies on the molecular recognition and binding characteristics in Rhodamine B molecularly imprinted polymer. *Journal of Lanzhou University (Natural Sciences) in Chinese, 39*(2), 57–60.

Wang, X., Wang, L. Y., He, X. W., Zhang, Y. K., & Chen, L. X. (2009). A molecularly imprinted polymer-coated nanocomposite of magnetic nanoparticles for estrone recognition. *Talanta, 78*, 327–332.

Xu, L. C., Pan, J. M., Dai, J. D., Li, X. X., Hang, H., Gao, Z. J., et al. (2012). Preparation of thermal-responsive magnetic molecularly imprinted polymers for selective removal of antibiotics from aqueous solution. *Journal of Hazardous Materials, 233–234*, 48–56.

Yamazaki, T., Ohta, S., Yanai, Y., & Sode, K. (2003). Molecular imprinting catalyst based artificial enzyme sensor for fructosylamines. *Analytical Letters, 36*(1), 75–89.

Yan, H. Y., Liu, B. M., Du, J. J., Yang, G. L., & Row, K. H. (2010). Ultrasound-assisted dispersive liquid–liquid microextraction for the determination of six pyrethroids in river water. *Journal of Chromatography A, 1217*, 5152–5157.

Yi, D. E., Lee, S. S., & Ying, J. Y. (2006). Synthesis and applications of magnetic nanocomposite catalysts. *Chemistry of Materials, 18*(10), 2459–2461.

Zhang, X. P., Chen, L. G., Xu, Y., Wang, H., Zeng, Q. L., Zhao, Q., et al. (2010). Determination of β-lactam antibiotics in milk based on magnetic molecularly imprinted polymer extraction coupled with liquid chromatography–tandem mass spectrometry. *Journal of Chromatography B, 878*, 3421–3436.

Zhang, Z. M., Tan, W., Hu, Y. L., & Li, G. K. (2011). Simultaneous determination of trace sterols in complicated biological samples by gas chromatography–mass spectrometry coupled with extraction using β-sitosterol magnetic molecularly imprinted polymer beads. *Journal of Chromatography A, 1218*, 4275–4283.